Sensor Applications

# Soft and Flexible Wireless Epidermal Plaster made by Laser-Induced Graphene

Alessio Mostaccio[1*], Federica Naccarata[1*], Francesca Maria Chiara Nanni[1*], Joanna Filippi[2], Eugenio Martinelli[2], and Gaetano Marrocco[1**]

[1] Pervasive Electromagnetics Lab, University of Rome Tor Vergata, Rome, RM 00133, Italy
[2] Bioinspired Electronic Engineering group, University of Rome Tor Vergata, Rome, RM 00133, Italy
[*] Student Member, IEEE
[**] Senior Member, IEEE

Manuscript received March 3, 2024; date of current version March 3, 2024.

Abstract—This paper introduces an epidermal antenna made of Laser-Induced Graphene (LIG) that is designed for hosting sensors within the UHF-RFID band (860-960 MHz). The upper bound performance is identified through numerical simulations and it is just 4 dB lower than a copper counterpart. Comparative assessments reveal that a significantly wider trace width is necessary to mitigate the intrinsic power loss of LIG.
Furthermore, the paper offers the first experimental demonstration of a LIG-based wireless flexible plaster, integrating a temperature-oriented RFID IC encapsulated between skin-friendly elastomers. To address impedance matching challenges, a small coupled aluminum loop is employed to interface with the RFID IC. The device underwent testing on volunteers across different body parts with varying curvatures. Results indicate an averaged realized gain of -19 dBi, enabling a potential biophysical parameter collection from distances of up to 35 cm using a 3.2 W Effective Isotropic Radiated Power (EIRP). This performance could support diverse applications in home care and sportswear. However, a notable efficiency degradation (5 dB) persists due to the interconnection of the antenna to the microchip transponder, presenting an ongoing challenge for optimization.

Index Terms—LIG, Flexible, Antenna, Polyimide, IoT, Wearable, Epidermal.

## I. INTRODUCTION

Epidermal electronics, in the form of light and flexible smart membranes [1], is the enabling technology that can provide the human skin with a two-way interface capable of capturing physical and chemical signals emitted by the body (temperature, sweat, and related analytes). Furthermore, this technology facilitates the digitalization of the body's interaction with the external environment, thereby restoring lost senses or introducing new ones, ultimately contributing to the emergence of the tactile internet [2]. Several applications are based on Radiofrequency Identification (RFID) in the HF (13.6 MHz) [3] and UHF (860-960 MHz) [4] bands.

Manufacturing techniques to deposit conducting patterns on skin-friendly substrates, enabling smart plasters with integrated sensing and radiating/backscattering capabilities, are spin coating, photolithography [5], sputtering [6], wire deposition [7], printing [8], and laser transferring [9].

However, as smart plasters are inherently disposable, their widespread adoption would demand for technologies that resort to eco-friendly substrates and minimize, or ideally reduce, the use of metallic conductive materials, thereby making manufacturing and waste recovery processes more sustainable. Conductive inks, containing metallic nanoparticles, are a suitable option for patterning electrical paths on flexible and eco-friendly materials. However, their sintering phase involving high temperatures either limits the choice of the substrate or enforces a multi-step process as in [10]. A promising alternative to copper/aluminum could be graphene, namely

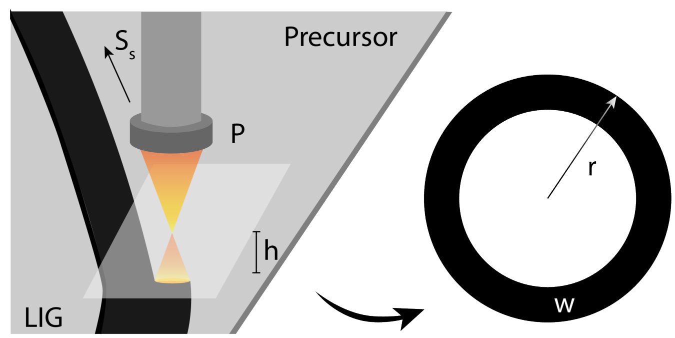


Fig. 1. Parameters of laser engraving to achieve graphene on a polyimide precursor and fabricate a loop antenna

a semiconductor with extraordinary chemical and physical properties [11]. Nevertheless, its large-scale application is currently impeded by the costly, time-consuming, and intricate chemical processes involved [11].

We will here explore the potentiality of fabricating RFID-based wireless epidermal sensors using the conversion of a polymeric substrate, referred as precursor [12], into a conductor through laser engraving to generate a graphene trace. This technique, known as LIG (Laser-Induced Graphene), leverages an infrared laser that induces a photo-thermal effect in the atomic structure of a polymeric precursor, such as Polyimide (PI) [12].

In principle, the sensor and the antenna could be scribed directly on the surface of the object (e.g., a medical-grade plaster) without resorting to aerosol jet printing technique [10], chemical etchants, or temperature-dependent bonding. Additionally, the possibility of scribing LIG onto low-cost and easily disposable substrates, such

Corresponding author: A. Mostaccio (e-mail: alessio.mostaccio@uniroma2.it).

Associate Editor:
Digital Object Identifier

TABLE 1. GEOMETRIC AND DIELECTRIC PARAMETERS @ 900 MHz OF THE BODY PHANTOM

| Layer | $\epsilon$ [-] | $\sigma$ [S/m] | t [mm] | Length [mm] | Width [mm] |
|---|---|---|---|---|---|
| *Skin* | 43.8 | 0.06 | 0.1 | 200 | 200 |
| *Fat* | 5.5 | 0.05 | 1 | 200 | 200 |
| *Muscle* | 54.5 | 0.06 | 10 | 200 | 200 |
| *Polyimide* | 3.5 | $10^{-15}$ | 0.125 | | |

as clothes, wood, and paper [12], could boost the development of eco-friendly epidermal devices.

So-obtained graphene has been extensively studied for manufacturing sensors, which, unlike epidermal wireless devices, are for the most interrogated with wired configurations [13].

Recently, LIG potentialities have been deeply investigated for their application to antennas with a special focus on UHF-RFID [14], [15].

The aim of this work is to *i*) identify the upper-bound radiation gain of epidermal UHF antennas made by LIG and the corresponding optimal size, and *ii*) provide the first experimental demonstration of a mostly conductor-free smart plaster made by LIG matched to an RFID IC and evaluate its performance when placed in some parts of the body.

## II. UPPER-BOUND PERFORMANCE

We will hereafter focus on a PI precursor assuming a sheet resistance of the produced graphene equal to $R_S = 10\ \Omega/\text{sq}$ which is a physically achievable value already demonstrated in [16]. Although lower values down to $0.3\ \Omega/\text{sq}$ have been reported in [17], they have not yet been reproduced by the authors, hence the aforementioned assumption can be regarded as conservative.

The reference antenna is a circular loop which is the shape that minimizes the overall size for a given efficiency [18]. We will preliminarily refer to the radiation gain, neglecting the impedance matching issue that will be instead addressed in the next section. In previous experiments involving epidermal antennas utilizing copper/aluminum, thin traces, and wires were often employed. However, in the case of laser-induced graphene, the conductivity is lower than that of regular conductors. Accordingly, we expect that the trace width will significantly impact the antenna gain since it is related to the loss resistance. The free geometrical parameters of the loop for a parametric exploration are the external radius $20 < r < 35$ mm and the width $2.5 < w < 10$ mm of the trace (Fig. 1). The loop is assumed to be placed on a layered planar model of the human body, incorporating muscle, fat, and skin. The device is simulated by Finite-Difference Time-Domain (FDTD) (CST Microwave Studio 2023). The graphene trace is accounted for by the surface impedance through the Leontovich condition [19].

Fig. 2a shows the simulated results relating the values of radiation gain vs. the loop parameters. As expected, the trace width is the most impacting parameter, especially for small radii ($r < 25$ mm). The optimal size is $r = 30$ mm and $w = 10$ mm, and the corresponding maximum radiation gain is $-14.5$ dBi. For the sake of comparison, the same analysis was also performed for a copper loop in the same arrangement (Fig. 2b). Even though the optimal form factor is practically identical to what found for LIG, and is coherent with [7], [18], the radiation gain is rather invariant to the width of the trace.

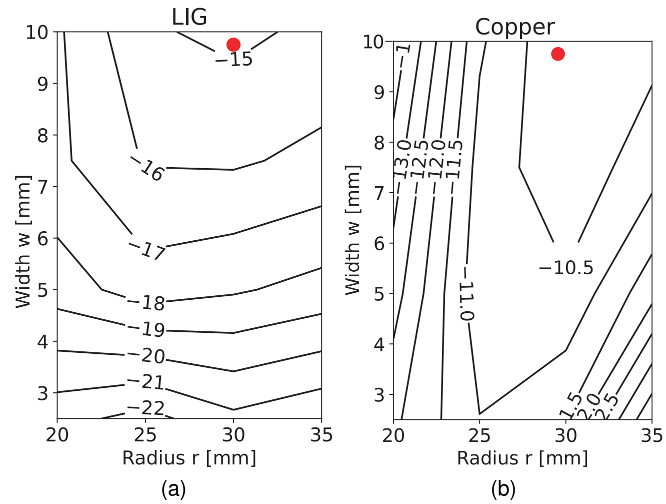


Fig. 2. Radiation gain at 900 MHz of LIG epidermal loop antenna w.r.t. to its outer radius and the track width for LIG (a) and copper (b) respectively. Red circles tag the optimal shape factor.

The comparison between the two materials indicates an efficiency loss of about 4 dB when moving from copper to LIG.

## III. PROTOTYPING AND TESTING

An experimental prototype of LIG-based epidermal included a temperature-oriented RFID IC, namely the Magnus S3 by Axzon [20], having power sensitivity $p_C = -13.6$ dBm and a nominal input admittance at 900 MHz $Y_C = 0.482 + j\omega C_{IC}$ mS. This IC is equipped with the capability of auto-tuning, i.e. it dynamically modifies its internal RF capacitance $C_{IC}$ to preserve a good impedance matching with the antenna and maximize the power collected by the IC even in case of deviation from nominal conditions during real applications [20]. The IC is also capable of temperature measurement in the range (−40°C, 85°C) with accuracy and precision for on-skin application equal to 0.25°C [4].

To achieve a conjugate impedance match of the LIG antenna to the IC, we resorted to the loop-match adapter [21], namely we introduced a second, much smaller rectangular loop that is inductively coupled to the LIG one (Fig. 3). We resorted to an aluminum adapter to avoid introducing further sources of power losses produced by the differential current mode that arises between the two loops. Moreover, to ease the manufacturing and the reproducibility, namely, to avoid soldering the IC to the graphene trace that would otherwise add contact resistances and, hence, additional losses, we carved the adapter out of a commercial off-the-shelf aluminum RFID tag (RFM3200-AER). The resulting size of the rectangular loop is 11.2 x 7.4 mm with a trace width of 1 mm. This arrangement also permits an easy repositioning of the adapter in repeated manufacturing and experimentation of LIG antennas. For comfortable placement on the skin, the two loops are hosted on a soft substrate of bio-compatible silicone ($\epsilon = 2.2$, $tan\delta = 0.005$ - Fig. 3). We introduced in the simulation the same IC impedance as before, thus neglecting the unpredictable difformity due to the specific soldering. When the highly lossy human body is involved as a host, the above approximation is expected to play a modest role in the overall performance of the antenna. The free parameters for the optimization of the power transfer coefficient ($\tau$) are the mutual distance $b$ and the thickness $d$ of silicon underneath.

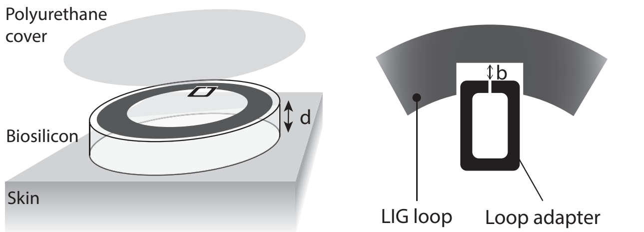


Fig. 3. Layout of the epidermal LIG antenna coupled with the aluminum adapter and its encapsulation with skin-friendly elastomers.

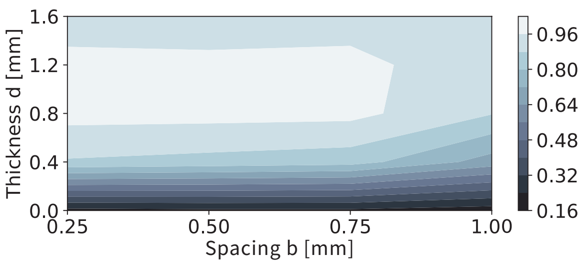


Fig. 4. Simulated power transfer coefficient ($\tau$) of the antenna system for different spacing $b$ between the adapter and the LIG loop, and thickness $d$ of the silicone layer.

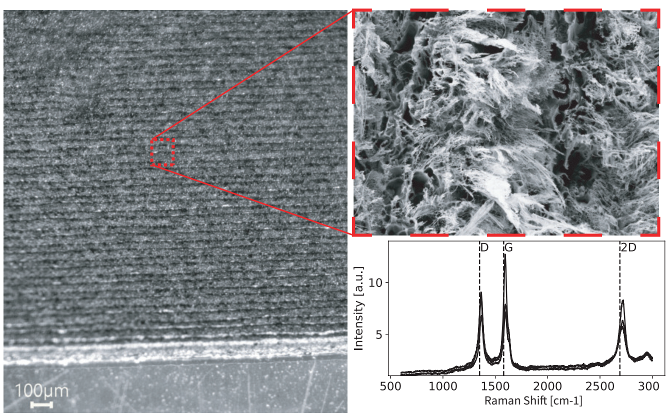


(a)

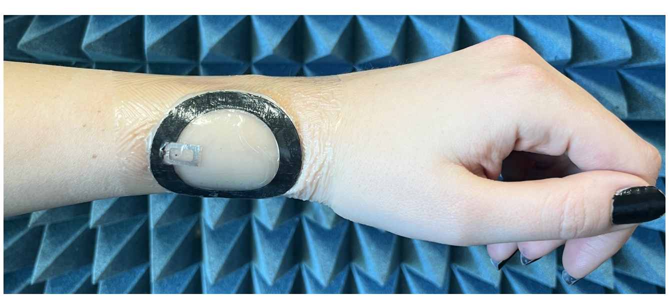

(b)

Fig. 5. (a) Magnification of LIG trace with stereomicroscopy and Field Emission Scanning Electron Microscopy (FESEM, Zeiss Leo Supra 35, with settings: Electron High Tension EHT= 5 kV and Working Distance WD=7 mm). Raman spectra in the inset. (b) Fabricated prototype of the epidermal sensor and application on the wrist of a subject.

Fig. 4 reports the value of power transfer coefficient $\tau$ at 900 MHz for different values of $\{b,\ d\}$. Overall a good matching ($\tau > 0.98$) can be achieved for a wide range of parameters. The selected configuration

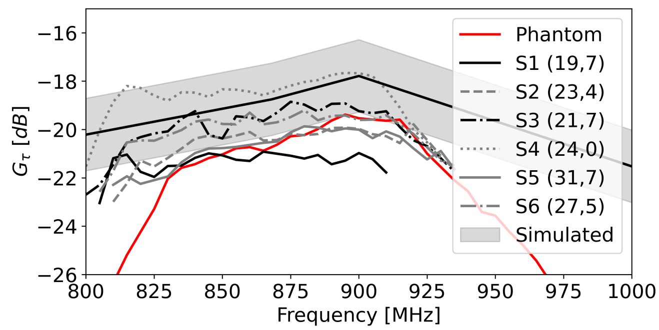


(a)

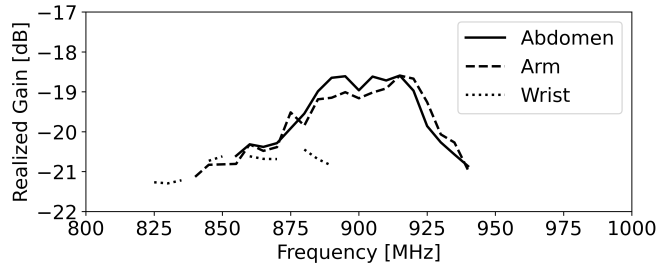


(b)

Fig. 6. (a) Comparison between measured and simulated realized gain of the LIG epidermal loop placed on the three-layer phantom and on the limb of 6 volunteers (Body Mass Index reported in brackets). (b) Measured realized gain in three body positions of subject S2 with different curvature, namely arm, abdomen, and wrist.

was $b = 250\ \mu m$ and $d = 0.8\ mm$.

The LIG layout was manufactured by a Trotec Speedy 100 Laser, which engraved the PI sheet (125 $\mu$m thick from DuPont) preliminary attached onto the silicone slab. The laser settings were borrowed from [16], namely a power $P = 9$ W, a scan speed $S_S = 10$ cm/s, and vertical offset of the beam focusing $h = 3$ mm. Accordingly, the engraving spots partially overlap to enhance the conductivity of the trace. The LIG patterning (shown in magnification in Fig. 5a) yielded a multilayer structure ($I_{2D}/I_G = 0.84$) that is defective for the most ($I_D/I_G = 0.99$) [16], with a sheet resistance of 12 $\Omega/sq$. The resulting device, (size $\{r, w\} = \{30\ mm, 10\ mm\}$), was hence positioned on the skin, with the antenna facing out of the body. It was fixed on the skin by a thin membrane (100 $\mu$m) of medical grade polyurethane (MPU) attached on top of the LIG antenna (see Fig. 5b) that protects the trace from potential damage caused by the unintentional contact with external objects. Detaching the MPU from the scribed LIG is expected to remove particles thus degrading the conductivity. Nevertheless, this will not impact real applications since the device can be intended for single use only.

The epidermal plaster was first evaluated by attaching it to a three-layered hydrogel-composed phantom (by AET, [22]) (size in Tab. 1) emulating muscle, fat, and skin. The realized gain was derived by the turn-on power, following the method in [7]. Measurements were repeated three times and averaged. Comparisons with the corresponding simulation are reported in Fig. 6a. Measured and simulated curves compare well, with less than 1 dB difference on average in the band of interest. However, the absolute value was slightly lower than the predicted upper bound in Fig. 2 with the LIG antenna only, possibly due to fabrication imperfections and, more significantly, to the matching loop inducing additional power

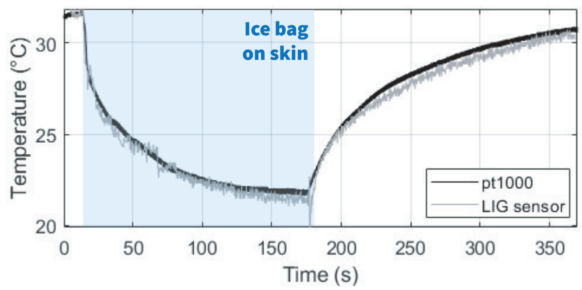


Fig. 7. Comparison between the temperature profile acquired with a PT1000 temperature sensor (black) and the proposed smart plaster (gray).

loss in the tissues. The robustness of the performance of the device was evaluated for applications on the abdomen of six volunteers aged between 25 to 35 y.o. (body mass index - BMI reported in the legend) (Fig. 6a). The gain remained relatively stable, showing an inter-person variation of ±1 dB.

Furthermore, to assess the antenna's performance concerning body curvature, the device was affixed to three different body portions of the same volunteer (labeled S2 in Fig. 6a), namely the abdomen (nearly flat surface), the arm (average curvature), and the wrist (high curvature). The gain response (Fig. 6b) is rather stable when moving from the abdomen to the arm. However, a more noticeable degradation was observed in the case of larger curvatures, particularly for high frequencies ($f > 890$ MHz), where the plaster did not respond to interrogations. Such degradation is probably related to the reduction of antenna performance due to the variation of its geometry. Instead, the LIG was already demonstrated to be robust versus bending [16].

Finally, to show an example of sensing, the skin was cooled with an ice bag and then left recovering to the basal temperature. A wired PT1000 thermocouple was also placed in the proximity of the IC for comparison. As shown in Fig. 7, the two responses are in good agreement during the entire thermal excursion with a root mean square error (RMSE) equal to 0.52°C.

## IV. CONCLUSION

The numerical analysis demonstrated that there exists an optimal size for epidermal LIG antennas in the RFID- UHF band, which is comparable to that of a good conductor counterpart. Due to the high sheet resistance of LIG, traces wider than the case of copper are necessary to mitigate losses. The impedance matching still remains however a critical issue since there is a not negligible efficiency degradation (nearly 5 dB) w.r.t. the upper-bound performance and will deserve a dedicated focus. Nevertheless, by considering 3.2 W EIRP of emitted power, the averaged measured realized gain (-19 dBi) in real placements on the body can afford a read distance of up to 35 cm. This still modest performance, can enable the monitoring of a user's physiological parameters in both supervised mode (using a handheld reader) and unsupervised mode, such as when the user passes through a gate/door. This functionality holds promising applications in home care and sportswear.

## V. ACKNOWLEDGMENTS

Work funded by European Union - NextGenerationEU, ECS 0000024 Rome Technopole, CUP B83C22002820006, PNRR Mission 4, Component 2, Investment 1.5.

## REFERENCES

[1] D.-H. Kim, N. Lu, R. Ma, Y.-S. Kim, R.-H. Kim, S. Wang, J. Wu, S. M. Won, H. Tao, A. Islam *et al.*, "Epidermal electronics," *science*, vol. 333, no. 6044, pp. 838–843, 2011.

[2] F. Naccarata, G. M. Bianco, and G. Marrocco, "Sensing performance of multi-channel rfid-based finger augmentation devices for tactile internet," *IEEE Journal of Radio Frequency Identification*, vol. 6, pp. 209–217, 2022.

[3] A. B. Barba, G. M. Bianco, L. Fiore, F. Arduini, G. Marrocco, and C. Occhiuzzi, "Design and manufacture of flexible epidermal nfc device for electrochemical sensing of sweat," in *2022 IEEE International Conference on Flexible and Printable Sensors and Systems (FLEPS)*. IEEE, 2022, pp. 1–4.

[4] C. Occhiuzzi, S. Parrella, F. Camera, S. Nappi, and G. Marrocco, "Rfid-based dual-chip epidermal sensing platform for human skin monitoring," *IEEE Sensors Journal*, vol. 21, no. 4, pp. 5359–5367, 2020.

[5] S. Davies, Y. Hu, N. Jiang, Y. Montelongo, A. Richardson, J. Blyth, and A. K. Yetisen, "Reversible photonic hydrogel sensors via holographic interference lithography," *Biosensors and Bioelectronics*, vol. 207, p. 114206, 2022.

[6] X. Wang, B. Zhong, Z. Lou, W. Han, and L. Wang, "The advancement of intelligent dressings for monitoring chronic wound infections," *Chemical Engineering Journal*, p. 149643, 2024.

[7] C. Miozzi, F. Amato, and G. Marrocco, "Performance and durability of thread antennas as stretchable epidermal uhf rfid tags," *IEEE Journal of Radio Frequency Identification*, vol. 4, no. 4, pp. 398–405, 2020.

[8] H. Chopra, I. Singh, T. B. Emran *et al.*, "Wearable technology based smart dressing for effective wound monitoring–correspondence," *International Journal of Surgery Open*, vol. 55, p. 100628, 2023.

[9] M. Farahani and A. Shafiee, "Wound healing: From passive to smart dressings," *Advanced Healthcare Materials*, vol. 10, no. 16, p. 2100477, 2021.

[10] S. Agarwala, G. L. Goh, T.-S. Dinh Le, J. An, Z. K. Peh, W. Y. Yeong, and Y.-J. Kim, "Wearable bandage-based strain sensor for home healthcare: Combining 3d aerosol jet printing and laser sintering," *ACS sensors*, vol. 4, no. 1, pp. 218–226, 2018.

[11] C. Soldano, A. Mahmood, and E. Dujardin, "Production, properties and potential of graphene," *Carbon*, vol. 48, no. 8, pp. 2127–2150, 2010.

[12] R. Ye, D. K. James, and J. M. Tour, "Laser-induced graphene," *Accounts of chemical research*, vol. 51, no. 7, pp. 1609–1620, 2018.

[13] L. Huang, J. Su, Y. Song, and R. Ye, "Laser-induced graphene: En route to smart sensing," *Nano-micro letters*, vol. 12, pp. 1–17, 2020.

[14] F. P. Chietera, R. Colella, A. Verma, E. Ferraris, C. E. Corcione, C. L. Moraila-Martinez, D. Gerardo, Y. H. Acid, A. Rivadeneyra, and L. Catarinucci, "Laser-induced graphene, fused filament fabrication, and aerosol jet printing for realizing conductive elements of uhf rfid antennas," *IEEE Journal of Radio Frequency Identification*, vol. 6, pp. 601–609, 2022.

[15] A. Mostaccio, G. Antonelli, R. Capuano, C. Di Natale, E. Martinelli, and G. Marrocco, "Full-lig wireless battery-less flexible sensor for the detection of triethylamine," *IEEE Journal on Flexible Electronics*, 2024.

[16] A. Mostaccio, G. Antonelli, M. Bragaglia, E. Martinelli, and G. Marrocco, "Comparative evaluation of laser induced graphene (lig) traces on polyimide under soft and hard stress for iot applications," *IEEE Journal on Flexible Electronics*, 2023.

[17] M. Tavakkoli Gilavan, M. S. Rahman, A. Minhas-Khan, S. Nambi, and G. Grau, "One-step fabrication of low-resistance conductors on 3d-printed structures by laser-induced graphene," *ACS Applied Electronic Materials*, vol. 3, no. 9, pp. 3867–3875, 2021.

[18] S. Amendola and G. Marrocco, "Optimal performance of epidermal antennas for uhf radio frequency identification and sensing," *IEEE Transactions on Antennas and Propagation*, vol. 65, no. 2, pp. 473–481, 2016.

[19] A. Mostaccio, A. Salvia, G. Antonelli, E. Martinelli, and G. Marrocco, "Upper bound performances of laser-induced graphene dipoles in the uhf band," in *2023 8th International Conference on Smart and Sustainable Technologies (SpliTech)*. IEEE, 2023, pp. 1–4.

[20] M. C. Caccami and G. Marrocco, "Electromagnetic modeling of self-tuning rfid sensor antennas in linear and nonlinear regimes," *IEEE Transactions on Antennas and Propagation*, vol. 66, no. 6, pp. 2779–2787, 2018.

[21] G. Marrocco, "The art of uhf rfid antenna design: Impedance-matching and size-reduction techniques," *IEEE antennas and propagation magazine*, vol. 50, no. 1, pp. 66–79, 2008.

[22] Human body equivalent phantom in low-frequency, microwave, and millimeter-waves, available online. Accessed: Feb. 6, 2024. [Online]. Available: https://www.aetassociates.com/pdf/electromagnetic.pdf